Supplementary material to the article

Double Nonstationarity: Blind Extraction of Independent Nonstationary Vector/Component from Nonstationary Mixtures — Algorithms

Zbyněk Koldovský, Václav Kautský, and Petr Tichavský

Acoustic Signal Analysis and Processing Group, Faculty of Mechatronics, Informatics, and Interdisciplinary Studies, Technical University of Liberec, Studentská 2, 461 17 Liberec, Czech Republic.
E-mail: zbynek.koldovsky@tul.cz, fax:+420-485-353112, tel:+420-485-353534

I. Extensions of Simulation Studies

A. Static Independent Component Extraction: Additional results for Section V-A.1

Fig. 8 shows the results of the experiment when $c = 0.5$, that is, when the SOI is Laplacean. Similarly to the experiment in the article, where the SOI is Gaussian ($c = 1$), the algorithms' performance is improved with growing α because the nonstationarity of the SOI improves the extraction. However, for a situation in which $\alpha \approx 0$, the SOI is non-Gaussian, and so the methods employing non-Gaussianity achieve ISR≤ -25; OGIVE$_{\mathbf{w}}$ does not achieve this accuracy level due to slow (therefore unfinished) convergence. The other non-Gaussianity-based algorithms (CSV-AuxIVE, FastDIVA/QuickIVE–rati–1 and FastDIVA/QuickIVE–rati–20) even slightly outperform FastDIVA/QuickIVE–gauss–20 for $\alpha \leq 1$; the latter algorithms rely only on the non-circularity of the SOI when $\alpha = 0$. LLJBD exploits neither higher-order nor non-circularity statistics and, therefore, it shows the behavior identical to when $c = 1$.

Fig. 9 shows the results for $c = 10$, that is, when the SOI distribution is sub-Gaussian. All algorithms' performance gets improved with growing α for values $\alpha > 1$, which shows that the strong nonstationarity is sufficient for successful extraction. This also holds for algorithms that assume non-Gaussianity, because strongly nonstationary (spiky) signals behave like super-Gaussian. For $\alpha \leq 1$, the algorithms behave in a way different from the previous versions of the experiment with $c = 0.5$ and $c = 1$. CSV-AuxIVE and QuickIVE-rati-1 fail (ISR is lower than 0 dB) for $\alpha \leq 1$. These methods cannot separate the sub-Gaussian SOI since the nonlinearities used in them are derived from super-Gaussian distributions. FastDIVA–rati–1 is different in this respect, as explained, e.g., in [1]. It can extract the sub-Gaussian SOI using a nonlinearity for super-Gaussian distribution due to automatic switching between maximization/minimization of the contrast function [1]. However, this property is not always guaranteed, especially when the signal model is not purely non-Gaussian. This can explain the loss in performance of FastDIVA–rati–1 when $0.4 < \alpha < 2$. In this interval, the histogram of the SOI is turning from a sub-Gaussian to a super-Gaussian shape due to the increasing nonstationarity. The fact that the algorithm fails in between (for $\alpha \approx 1$) is in agreement with the explanation provided in [2]. Similar behavior and its explanation hold for FastDIVA–rati–20 (which fails for $\alpha \approx 0.6$).

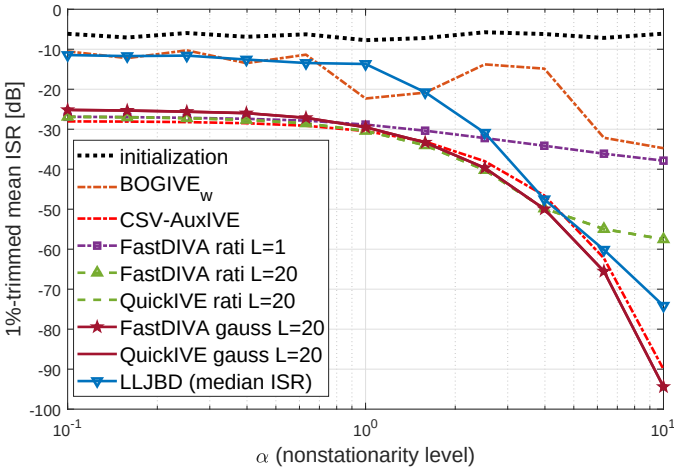

Fig. 8. Resulting ISR as a function of α when $c = 0.5$, i.e., the SOI is Laplacean; the circularity coefficient is $\delta = 0.5$.

LLJBD and FastDIVA/QuickIVE–gauss–20 are not affected by the non-Gaussianity of the SOI and perform more or less similar to $c = 0.1$ and $c = 1$. The latter variants proposed in this paper achieve the same performance, which is the best among the compared methods in this setting.

B. Dynamic Independent Component Extraction: Additional results for Section V-A.2

The experiment of Section V-A.2 with Gaussian SOI is here repeated with $c = 0.5$, that is, when the SOI is Laplacean. The results are shown in Fig. 10. As could be foreseen, the results confirm that all the methods employing the non-Gaussianity

[0]This work was supported by The Czech Science Foundation through Project No. 20-17720S and by the United States Department of the Navy, Office of Naval Research Global, through Project No. N62909-19-1-2105.

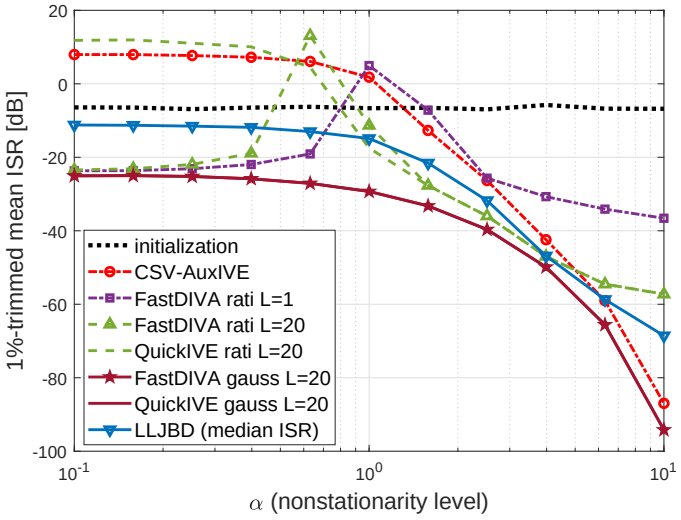

Fig. 9. Resulting ISR as a function of α when $c = 10$, i.e., the SOI has sub-Gaussian distribution; the circularity coefficient is $\delta = 0.5$.

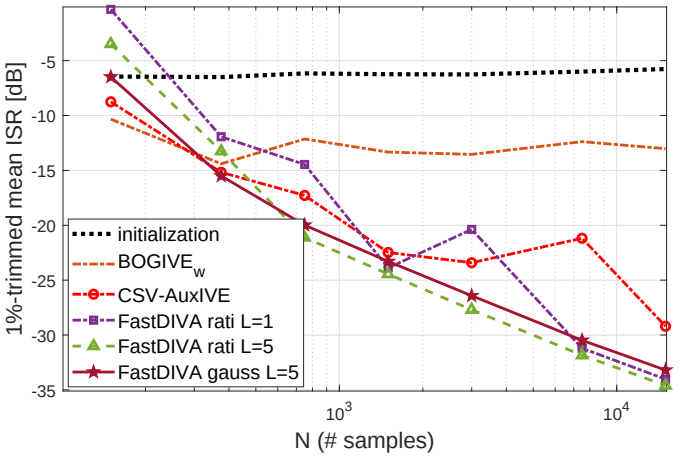

Fig. 10. ISR as a function of the length of data N when $c = 0.5$ and $\delta = 0.5$ (Laplacean noncircular SOI), $T = 3$ (nonstationary CSV mixing model), and $L = 5$ and $\alpha = 2$ (nonstationary source model). N ranges from 150 through $15,000$; the length of sub-blocks $N_s/(TL)$ thus ranges from 15 through $1,000$.

(BOGIVE$_\mathbf{w}$, CSV-AuxIVE, FastDIVA–rati–1, and FastDIVA–rati–5) achieve ISR, which is considerably better than that valid for $c = 1$ (Gaussian SOI). BOGIVE$_\mathbf{w}$ shows poor performance due to unfinished convergence (with the number of iterations limited to $1,000$). For $N > 400$, FastDIVA–rati–5 slightly outperforms FastDIVA–Gauss–5 thanks to more accurate capturing of the non-Gaussianity and nonstationarity of the SOI. However, it is less accurate for $N \leq 400$, which points to a higher robustness of the latter approach to the lack of available data.

C. Independent Vector Extraction: Additional results for Section V-A.3

For the same setting ($K = 5$, $T = 1$, $\alpha = 2$, $c = 0.5$, $\delta = 0.5$, $L = 10$, $N = 500$), Fig. 11 shows mean ISR achieved by the algorithms in $1,000$ trials as a function of the dimension d. The compared algorithms are tested in two regimes in which

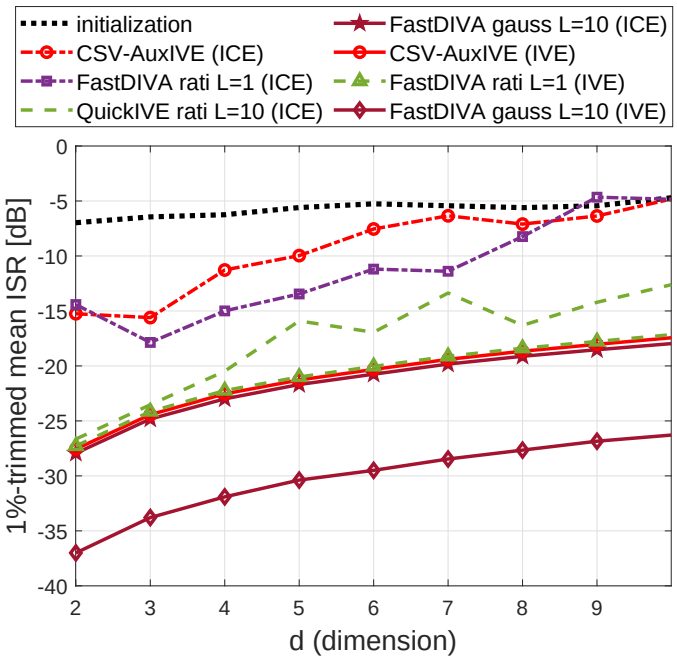

Fig. 11. Comparison of separate (ICE) and joint (IVE) blind extraction: ISR as a function of the dimension d. The parameters of the experiment are $\alpha = 2$, $c = 1$, $\delta = 0.5$, $L = 10$ (nonstationary Gaussian noncircular SOI), $T = 1$ (static mixtures), $K = 5$ (five jointly dependent mixtures per trial), and $N = 500$.

the K mixtures are processed (ICE) separately and (IVE) jointly.

In the ICE regime, the algorithms achieve sub-optimal performance levels since the dependencies among the SOI components are not used. They show less stable convergence in the sense that there are more cases in which a source different from the SOI is extracted. FastDIVA–rati–10 has often failed to extract the SOI in this setting (not shown in Fig. 11); QuickICE–rati–10 appears to be more stable. Only FastDIVA–gauss–10 yields stable performance in the ICE regime.

In the IVE regime, these methods show a substantially better stability as well as accuracy levels. The best extraction accuracy is achieved by FastDIVA–gauss–10 in the IVE regime.

The fact that the performance of the algorithms in Fig. 11 is getting worse with the growing dimension d might seem to be questionable at first sight. It means that the ISR is getting worse when more inputs (sensors) are provided. This is, nevertheless, in good agreement with the Cramér-Rao theory where the lower bounds for the achievable ISR through ICA/IVA/ICE/IVE/CSV typically grow linearly with d; see, e.g., [3]–[7]. However, this phenomenon need not occur when working with real-world measurements, which involve various sources of noise and interference whose number can be higher than d. Such real-world data does not obey the determined mixing condition: The background subspace has the full dimension d as opposed to $d - 1$. Therefore, the extraction accuracy achieved for real-world measurements is typically improved with the growing number of inputs d; see, e.g., [8].

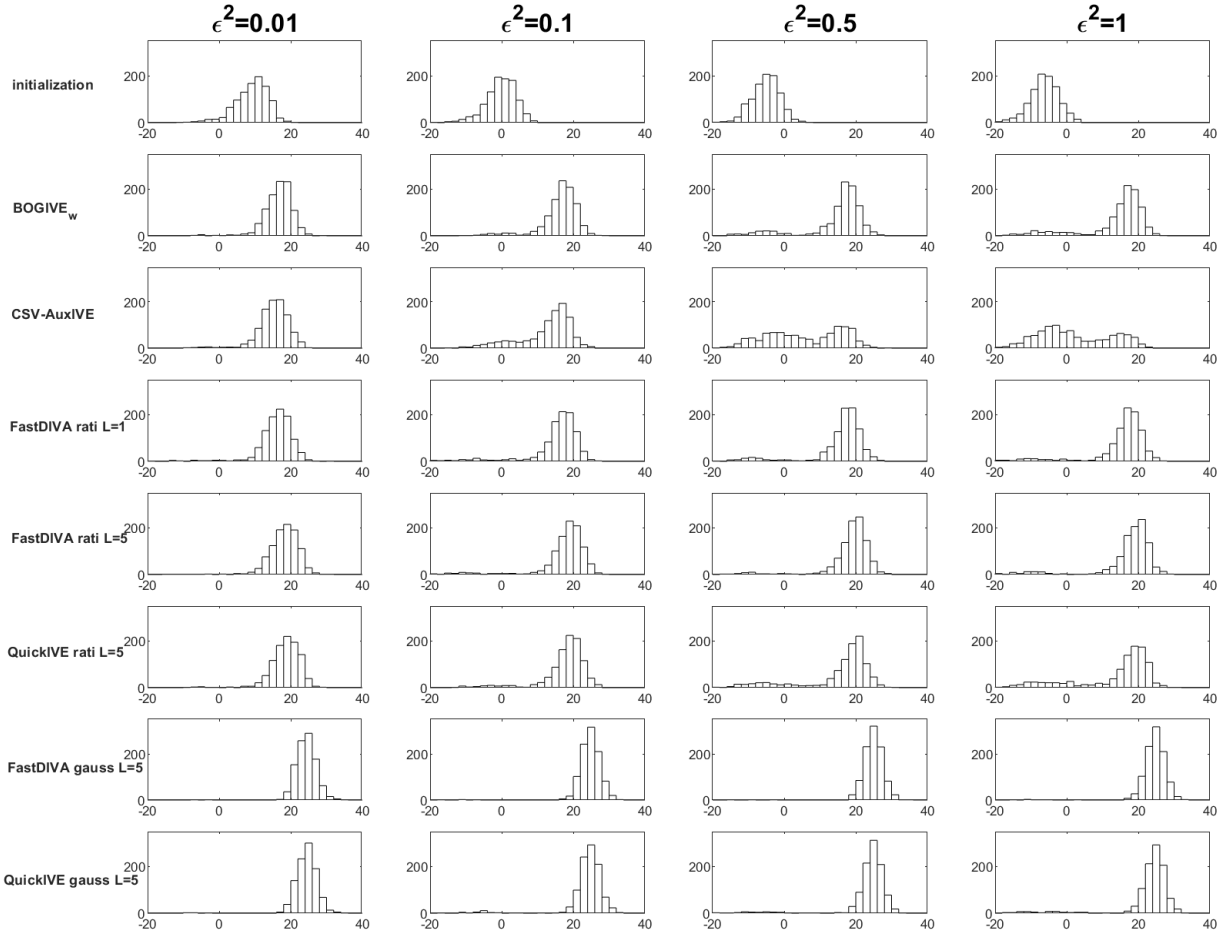

Fig. 12. Histograms of Signal-to-Interference-Ratio (SIR) shown for different values of perturbation of the initialization ϵ^2; the results correspond to the variant of the experiment when the background signals are circular Gaussian. SIR higher than 0 dB means that the algorithm converged to the SOI and vice versa.

D. Domain of Attraction of the SOI

Here, the experiment from Section V-A.2 is repeated ($K = 1$, $T = 3$, $L = 5$, $N = 1000$, $d = 6$, $\alpha = 2$, $c = 1$, $\delta = 0.5$) when the norm of the initial perturbation vector $\epsilon^2 = \|\boldsymbol{\epsilon}_k\|^2$ varies from 0.01 through 1. For each value of ϵ^2, 1000 trials are done and the histogram of ISR achieved by the given algorithm is shown. The experiment is realized in two variants when the background signals are (1) circular Gaussian (Fig. 12), and (2) circular Laplacean (Fig. 13). Any BSE algorithm is expected to converge to the SOI (achieve "small" ISR) when it is initialized in the close vicinity of the true separating vector. It can converge to a different source (achieve "high" ISR) when it is initialized in the domain of attraction of a different source than the SOI. The latter case is more probable when ϵ^2 is high. This experimental evaluation has been proposed in [9].

Fig. 12 shows that the variants of FastDIVA and QuickIVE are highly robust to the initialization when the background signals are circular Gaussian. This is because the contrast function has only one significant global optimum point corresponding to the SOI. The other local extremes are rather flat to attract these methods. The gradient-based BOGIVE$_{\mathbf{w}}$ and CSV-AuxIVE show higher sensitivity to the local extremes.

Fig. 13 shows a more realistic situation, that is, when the background signals involve other non-Gaussian (Laplacean) sources, which have wider domains of attraction, so the compared algorithms are much more sensitive to ϵ^2 than in the previous case. FastDIVA–gauss–m and QuickIVE–gauss–m show very good global convergence in this setting, which is obviously caused by the matched SOI source model. We can conclude that choosing an accurate estimate of the score function of the SOI may be a way to improve the global convergence of the proposed algorithms.

REFERENCES

[1] Z. Koldovský, V. Kautský, T. Kounovský, and J. Čmejla, "Algorithm for independent vector extraction based on semi-time-variant mixing model," 2021.

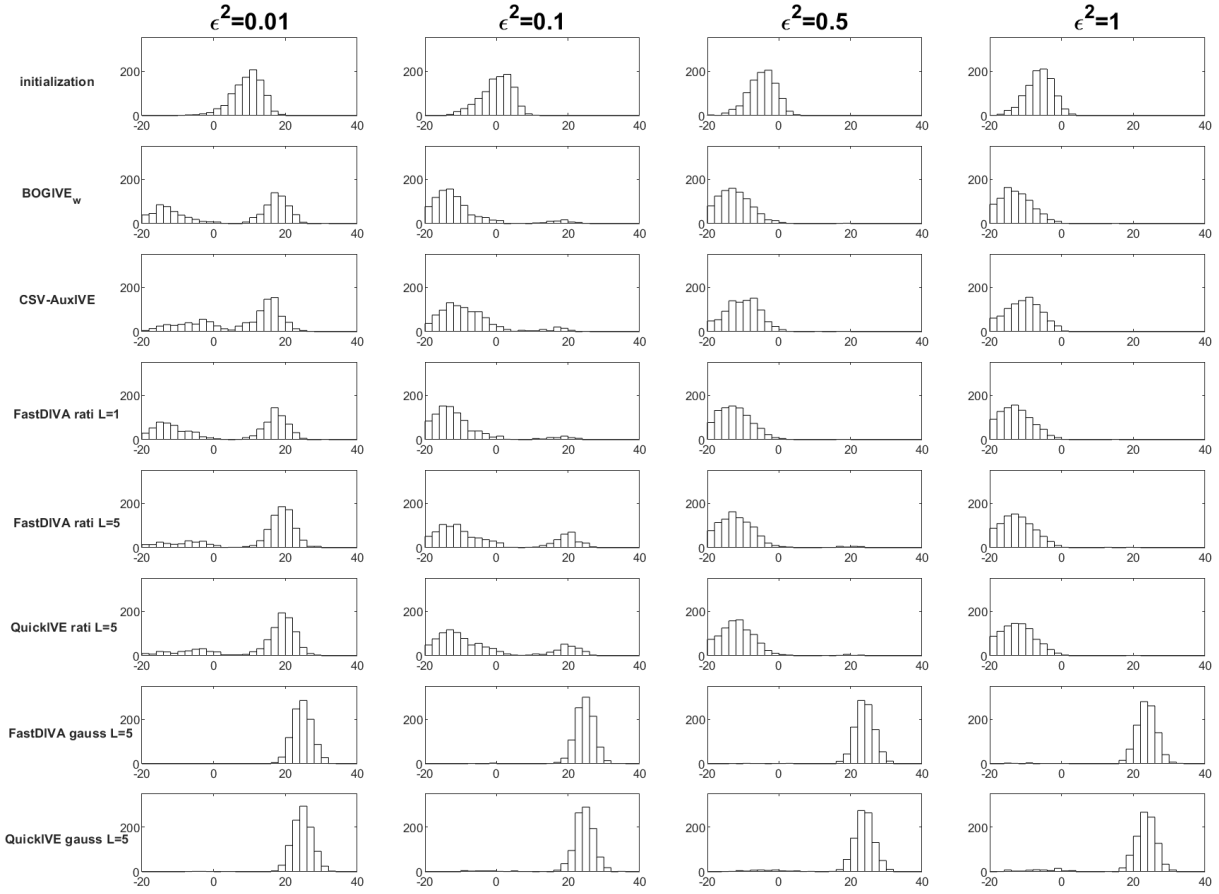

Fig. 13. Histograms of Signal-to-Interference-Ratio (SIR) shown for different values of perturbation of the initialization ϵ^2; the results correspond to the variant of the experiment when the background signals are circular Laplacean. SIR higher than 0 dB means that the algorithm converged to the SOI and vice versa.

[2] P. Tichavský, Z. Koldovský, and E. Oja, *Speed and Accuracy Enhancement of Linear ICA Techniques Using Rational Nonlinear Functions*. Berlin, Heidelberg: Springer Berlin Heidelberg, 2007, pp. 285–292.

[3] P. Tichavský, Z. Koldovský, and E. Oja, "Performance analysis of the FastICA algorithm and Cramér-Rao bounds for linear independent component analysis," *IEEE Transactions on Signal Processing*, vol. 54, no. 4, pp. 1189–1203, April 2006.

[4] B. Loesch and B. Yang, "Cramér–Rao bound for circular and noncircular complex independent component analysis," in *IEEE Trans. Signal Processing*, vol. 61, Jan 2013, pp. 365–379.

[5] M. Anderson, G. Fu, R. Phlypo, and T. Adalı, "Independent vector analysis: Identification conditions and performance bounds," *IEEE Transactions on Signal Processing*, vol. 62, no. 17, pp. 4399–4410, Sept 2014.

[6] V. Kautský, P. Tichavský, Z. Koldovský, and T. Adalı, "Performance bounds for complex-valued independent vector analysis," *IEEE Transactions on Signal Processing*, vol. 68, pp. 4258–4267, 2020.

[7] V. Kautský, Z. Koldovský, P. Tichavský, and V. Zarzoso, "Cramér–Rao bounds for complex-valued independent component extraction: Determined and piecewise determined mixing models," *IEEE Transactions on Signal Processing*, vol. 68, pp. 5230–5243, 2020.

[8] Y. Kubo, N. Takamune, D. Kitamura, and H. Saruwatari, "Blind speech extraction based on rank-constrained spatial covariance matrix estimation with multivariate generalized gaussian distribution," *IEEE/ACM Transactions on Audio, Speech, and Language Processing*, vol. 28, pp. 1948–1963, 2020.

[9] Z. Koldovský and P. Tichavský, "Gradient algorithms for complex non-gaussian independent component/vector extraction, question of convergence," *IEEE Transactions on Signal Processing*, vol. 67, no. 4, pp. 1050–1064, Feb 2019.